UNIVERSITE BLAISE PASCAL IN2P3

LABORATOIRE DE PHYSIQUE CORPUSCULAIRE

63177 AUBIERE CEDEX

TELEPHONE : 73.26.41.10
TELECOPIE : 73.26.45.98

PCCF - RI -- 90-02


J.P. ALARD, F. BIAGI, P. MOREL, N. BASTID, J. AUGERAT, P. CHARMENSAT, M. CROUAU, P. DUPIEUX, L. FRAYSSE, J. MARRONCLE, G. MONTAROU, M.J. PARIZET, D. QASSOUD, A. RAHMANI.

LPC CLERMONT, IN2P3 - CNRS, Université Blaise Pascal
F-63177 AUBIERE CEDEX, FRANCE

R. BABINET, Z. FODOR, J. GIRARD, J. GOSSET, D. L'HOTE, B. LUCAS, J. POITOU, W. SCHIMMERLING, Y. TERRIEN, O. VALETTE.

DPHN Saclay, F-91191 Gif-sur Yvette Cedex - FRANCE

M.C. LEMAIRE - LNS Saturne, F-91191 Gif-sur Yvette Cedex - FRANCE

F. BROCHARD, P. GORODETZKY, C. RACCA

CRN Strasbourg, F-67037 Strasbourg Cedex - FRANCE

# LIGHT FRAGMENT PRODUCTION AT FORWARD ANGLES IN Ne AND Ar INDUCED REACTIONS

JOURNEES DES THEORICIENS SATURNE.3, JTS 3

23-24 Novembre 1989 - SACLAY

PCCF RI 9002

# LIGHT FRAGMENT PRODUCTION AT FORWARD ANGLES IN Ne AND Ar INDUCED REACTIONS

J.P. Alard, F. Biagi, P. Morel, N. Bastid, J. Augerat, P. Charmensat,
M. Crouau, P. Dupieux, L. Fraysse, J. Marroncle, G. Montarou,
M.J. Parizet, D. Qassoud, A. Rahmani.

L.P.C. Clermont, F 63177 Aubière Cedex

R. Babinet, Z. Fodor, J. Girard, J. Gosset, D. L'Hote, B. Lucas,
J. Poitou, W. Schimmerling, Y. Terrien, O. Valette.

DPHN Saclay, F 91191 Gif-sur-Yvette Cedex

M.C. Lemaire.

LNS Saturne, F 91191 Gif-sur-Yvette Cedex

F. Brochard, P. Gorodetzky, C. Racca.

CRN Strasbourg, F 67037 Strasbourg Cedex

## I)-Introduction.

Fragment emission at small angles in nucleus-nucleus collisions is a topic of current interest. With the Bevalac accelerator at the LBL, inclusive experiments using beams of protons, deuterons, alpha particles and carbon nuclei (E/A = 0.4 GeV, 1.05 GeV and 2.1 GeV) on C, Ca, Pb and $CH_2$ targets have been performed [1]. Some studies about projectile fragmentation, obtained with smaller incident energies, were recently performed at GANIL [2] (Argon beams of E/A = 26.5 and 44 MeV on various targets) and SARA [3] (C, N, Ne beams of E/A = 30 MeV on various targets).

At Saturne, the Diogene plastic wall [4] has been used to investigate light fragment emission at small angles, in both peripheral and non peripheral nuclear collisions, using different selected multiplicities in the central chamber. For the first time, the results of such exclusive measurements are reported in the present paper, both for Ne and Ar projectiles on various targets.

Let us note that more complete exclusive measurements, using heavier projectile nuclei, will be performed later with the $4\pi$ facility actually in progress at SIS/ESR [5].

## II)- Experimental set up and performances.

The Plastic wall associated with the Diogene pictorial drift chamber [4] is made up of two parts: the internal wall (at 5.57 m from the target) for the detection of fragments

emitted in the angular range $0^0$ - $2^0$ and the external wall (at 4.11 m from the target) for the detection of fragments emitted in the angular range $2^0$ - $5^0$.

Fig 1 shows the general structure of the Diogene Plastic Wall. The internal wall is a 4x4 array of two scintillator telescopes (NE 110A). The external wall is made up of four identical quadrants; each quadrant is a set of height position sensitive telescopes. Each of them consists of two 96x8x2 $cm^3$ slabs of NE 110 scintillator, viewed at one end by a photomultiplier. The two phototubes, at opposites ends of the telescopes, are operated in coincidence in order to reduce the background. The time difference between the two photomultipliers is a measurement of the position along the couple of slabs. (resolution 4 cm FWHM). The detection treshold is about 350 MeV/c for protons.

For the two parts of the wall, the charge distribution of the fragments is obtained from the correlation between the energy loss in the scintillators and the time of flight [6]. In the internal wall charges 1 to 7 are easily identified ( see fig 2). On the external wall, only charges 1 to 3 are recorded.

The emission angle of fragments detected in the plastic wall is obtained with an uncertainty of 0.7 degree and the time of flight with an uncertainty of 400 ps, which corresponds, for protons, to $\Delta p/p$ = 4.2 % at p = 1 GeV/c and $\Delta p/p$ = 8.5 % at p = 1.5 GeV/c (FWHM).

The data reported here correspond to Ne and Ar projectiles. For the Ne projectiles, we have a selection on non peripheral events by requiring in the trigger that at least 2 particles were measured in the chamber at angles between $37^0$ and $119^0$ with an energy above 43 MeV for pions and 70 MeV for protons.

Fig 2 shows an example of identification of charges in the internal wall in the case of Ne projectiles.

## III)- EXPERIMENTAL RESULTS.

### III-1-Correlation between zero-degree and large angle multiplicities.

In fig 3 we present the variation of the mean multiplicity in the central chamber versus the total charge $Z_{TOT}$ detected in the plastic wall, for Neon projectiles on NaF and Pb targets at E/A = 400 and 800 MeV.

In fig 4 we present the same study for Argon projectiles on Ca, Nb, Pb targets, for incident energies from 200 to 600 A.MeV.

In all cases, we observe a strong anticorrelation between the two quantities. This indicates that $Z_{TOT}$ can also be used alternately with $N_c$ to specify the impact parameter selection.

At both beam energies the anticorrelation is stronger for heavy targets, and the effect is more pronounced at high energy. Such effects are at least qualitatively in agreement with the participant-spectator picture.

### III-2-Double differential cross sections.

Differential cross sections for light fragments have been measured at several angles. We present here a few typical results, mainly the data concerning Z = 1 fragments. The

velocity spectra are transformed into p/A distributions, assuming that all particles are baryons, thus neglecting pion production.

The momentum distribution of Z = 1 fragments is presented fig 5 - 6 for Ne + Pb at E/A = 400 MeV and for Ar + (Ca, Nb) at E/A = 400 MeV, at 3 degrees without any cut on multiplicity in the central chamber. We can made the following observations:

(i) The projectile fragmentation peak is approximately at the same momentum as the projectile. No slowing down can be seen.

(ii) At lower values of the momentum per nucleon there is a clear excess of counts with respect to the extrapolation of the fragmentation peak, which can be attributed to particles emitted from the participant region.

In fig 7 we present as an example the same spectra for Ar + Ca at 400 A.MeV for Z = 3 fragments. There is essentially one peak at the same momentum per nucleon as the beam.

In fig 8 we present the momentum distribution of Z = 1 fragments around $3^0$ in Ne (E/A = 400 MeV) + Pb collisions in coincidence with higher and higher multiplicities $N_c$ in the central chamber. The fragmentation peak is strongly dominant for strong multiplicities. At high multiplicity the fragmentation component is still present, which might be interpreted as some transparency of the Pb nucleus for central collisions.

On the contrary for NaF target the fragmentation peak dominates even for the larger multiplicities; in fact, nucleons at the edge of the projectile do not go through a thick piece of nuclear matter from the target.

Similar observations can be made with Argon projectiles.

IV)- Analysis with a two source model.

The principle of such an analysis has been described elsewhere [7]. We have used a simple thermodynamical model in order to describe the shape of the experimental spectra obtained for Z = 1 fragments. Calculated spectra are obtained by the superposition of two components : one corresponding to the participant zone, and the other one corresponding to the projectile remnant. For each component, we use 4 parameters: the density, the temperature, the velocity of the source and a normalization factor. The momentum distribution is taken as a Fermi distribution:

$$d^2\sigma/dP.d\Omega = K.\rho^{-1}.p^2.E^{-1}\gamma(E - \beta p\cos\theta)$$

$$x[\exp((\gamma(E - \beta p\cos\theta) - \mu)/T) + 1]^{-1}$$

where p is the momentum, E the total energy, $\theta$ the laboratory angle. $\beta$ is the velocity of the source and $\gamma$ the corresponding Lorentz factor. T is the temperature and $\mu$ is the chemical potential at nuclear density $\rho$. K is a parameter which contains the number of nucleons of the source.

COMPARISON WITH EXPERIMENTAL DATA: A typical example of comparison is shown in fig 9 for Pb and NaF targets for 800 A.MeV projectiles. Another example is given on fig 10 for Ar projectiles on Nb at 400 A.MeV. Extracted temperatures for the projectiles are given in table I for both Ne and Ar projectiles. We can make the following observations concerning the temperatures associated with the projectile fragments:

(i) The temperature increases as incident energy increases (larger energy transfer to the projectile remnant at higher incident energies)

(ii) The temperature increases as the impact parameter decreases (stronger abrasion for small impact parameters)

(iii) The temperature increases as the mass of the projectile increases (larger energy transfer, stronger abrasion effects). We note that it is the first time that we can put in evidence such a phenomena.

Concerning the temperature of the participant zone, its value is about several tenths of MeV. It is difficult to make a systematic study because of the lack of statistics, and because of the effect of the low momentum cut of the wall. A more precise and complete study of the hadronic temperature in the participant zone has been made with the particles detected in the central chamber of Diogene [8].

It must be noted that the extracted temperatures should be only considered as approximate temperatures because we have assumed thermal equilibrium and no velocity distributions in the sources.

In conclusion, we have presented experimental results obtained with the Diogene Plastic Wall in the angular range $0^0 - 5^0$ in the laboratory system, for light fragments emitted in Ne and Ar induced reactions. There are strong correlations between multiplicities measured at large angles and at small angles, which can be used particularly for heavy targets, to select peripheral from central events. On the other hand, the velocity spectra of Z = 1 fragments seems to put in evidence some transparency effects, and shows the existence of two sources : the projectile remnant at the beam velocity and the participant region at intermediate velocity. Such results are in good agreement with the participant spectator model.

**Temperatures extracted from Ar and Ne induced reactions in MeV**

| Angle | $1^o$ | $3^o$ | $5^o$ |
|---|---|---|---|
| Ar + Ca (400 A.MeV) | 4.33 ± 0.07 | 4.62 ± 0.04 | 6.88 ± 0.09 |
| Ar + Nb (400 A.MeV) | 4.32 ± 0.15 | 5.35 ± 0.13 | 11.02 ± 0.18 |
| Ar + Ca (600 A.MeV) | 5.35 ± 0.06 | 8.87 ± 0.08 | 12.60 ± 0.11 |
| Ar + Nb (600 A.MeV) | 6.05 ± 0.20 | 9.94 ± 0.34 | 13.47 ± 0.40 |
| Ne + NaF (400 A.MeV) | — | 4.4 ± 0.1 | — |
| Ne + Pb (400 A.MeV) | — | 4.7 ± 0.2 | — |
| | | | |
| Ar + Ca (400 A.MeV) | Central collisions, | all angles | 8.82 ± 0.25 |
| | Mean collisions, | all angles | 6.19 ± 0.08 |
| | Peripheral collisions, | all angles | 4.75 ± 0.03 |

**Table I**

## References


1) L. Anderson et al, Phys. ReV. C28 (1983) 1224

2) D. Guerreau et al, Phys. Lett. 131B (1983) 293

3) D. Guinet et al , Phys. Lett. 137B (1984) 318

4) J.P. Alard et al, Nucl. Inst. Methods A261 (1987) 379

5) Proposal from the $4\pi$ collaboration at GSI, "Composite particle production in central and semi central collisions of Au on Au", May 1989

6) N. Bastid, Thesis, Clermont-Ferrand (1987) unpublished

7) N. Bastid et al, Nucl. Physics, to be published.

8) M.J. Parizet et al, Int. Journ. of Mod. Phys A, vol4, 14 (1989) 3689

## Figures captions

Fig 1 : The structure of the Diogene Plastic Wall.

Fig 1 : An example of identification of charges in the internal wall.

Fig 3 : Anticorrelation between the total charge in the wall and the charged multiplicity in the chamber, for Ne + NaF (aquares) and Ne + Nb ( circles) collisions, at 400 A.MeV (left) and 800 A.MeV (right).

Fig 4 : The same anticorrelation for Argon + Nucleus collisions.

Fig 5 : Double differential cross section for Z = 1 fragments in Ne + Pb collisions at 800 A.MeV incident energy. The arrow indicates the momentum per nucleon of the Neon beam.

Fig 6 : The same differential cross sections for an Argon beam.

Fig 7 : The same differential cross sections for an Argon beam and Z = 3 fragments in the inner wall.

Fig 8 : variation of the momentum spectra with the centrality of the collision, showing the effect of the transparency of the nuclear matter.

Fig 9 : A thermodynamical fit of the differential cross section, with a two sources model as described in the text, for Ne + Nb at 400 MeV (a) and 800 MeV (b) incident energy.

Fig 10 : The same differential cross section for Argon projectiles.

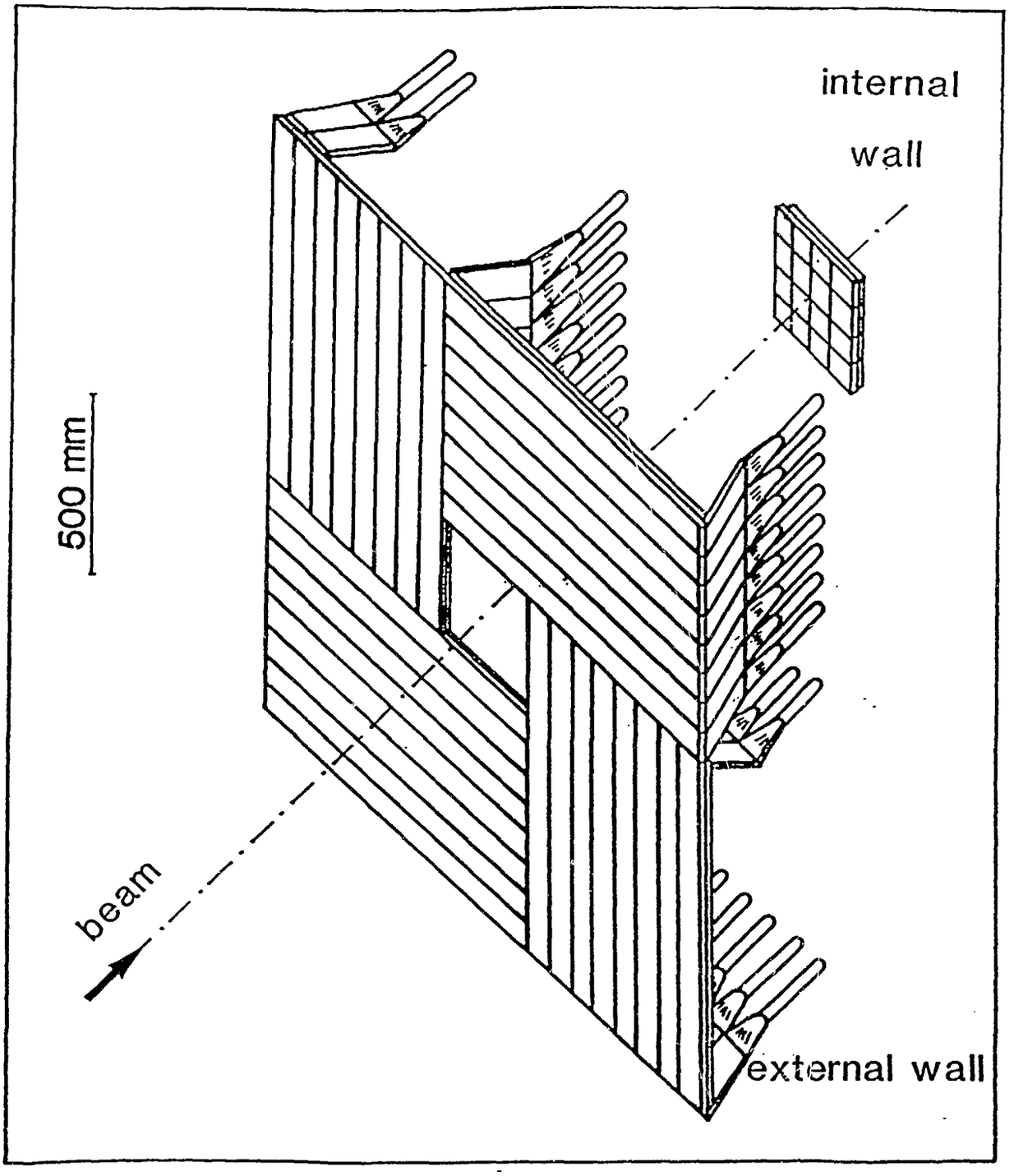


FIG.1

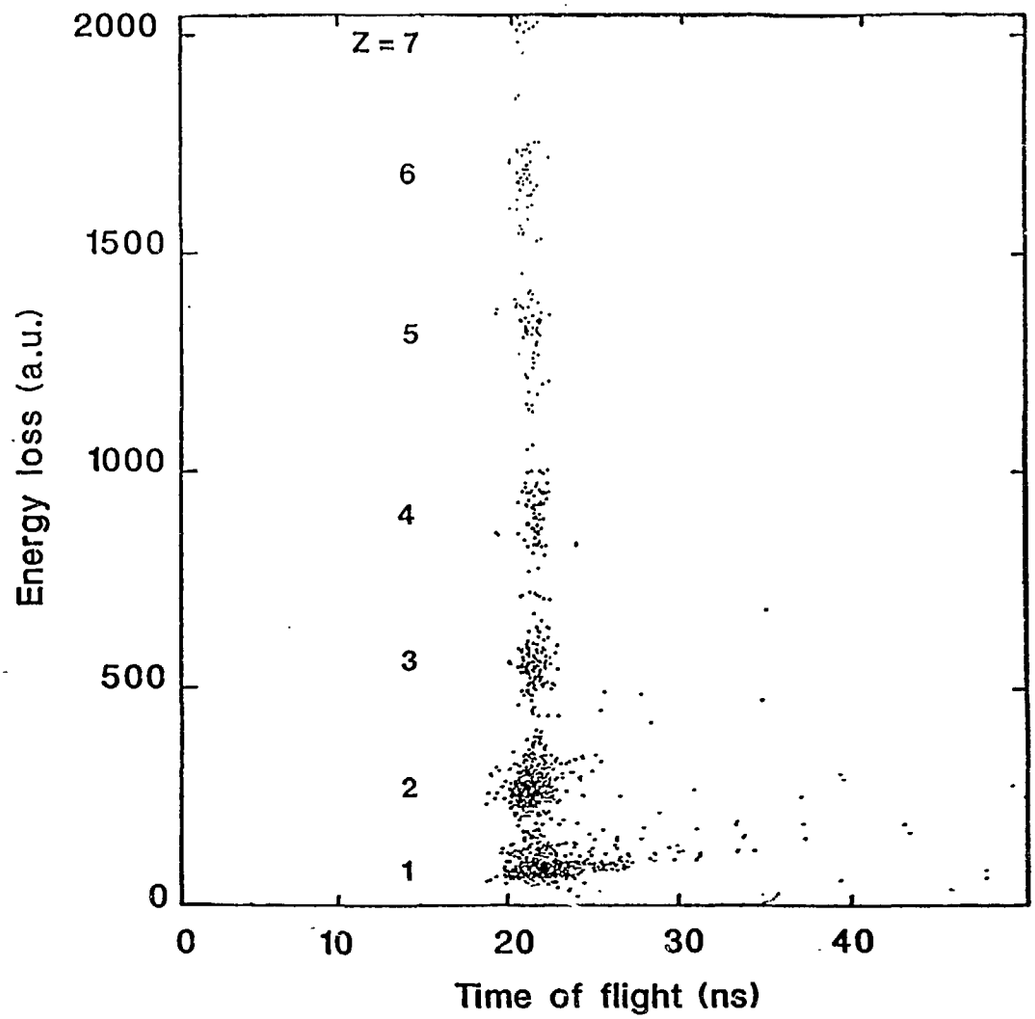
2000
1500
1000
500
0
Energy loss (a.u.)
Z = 7
6
5
4
3
2
1
0
10
20
30
40
Time of flight (ns)

FIG.2

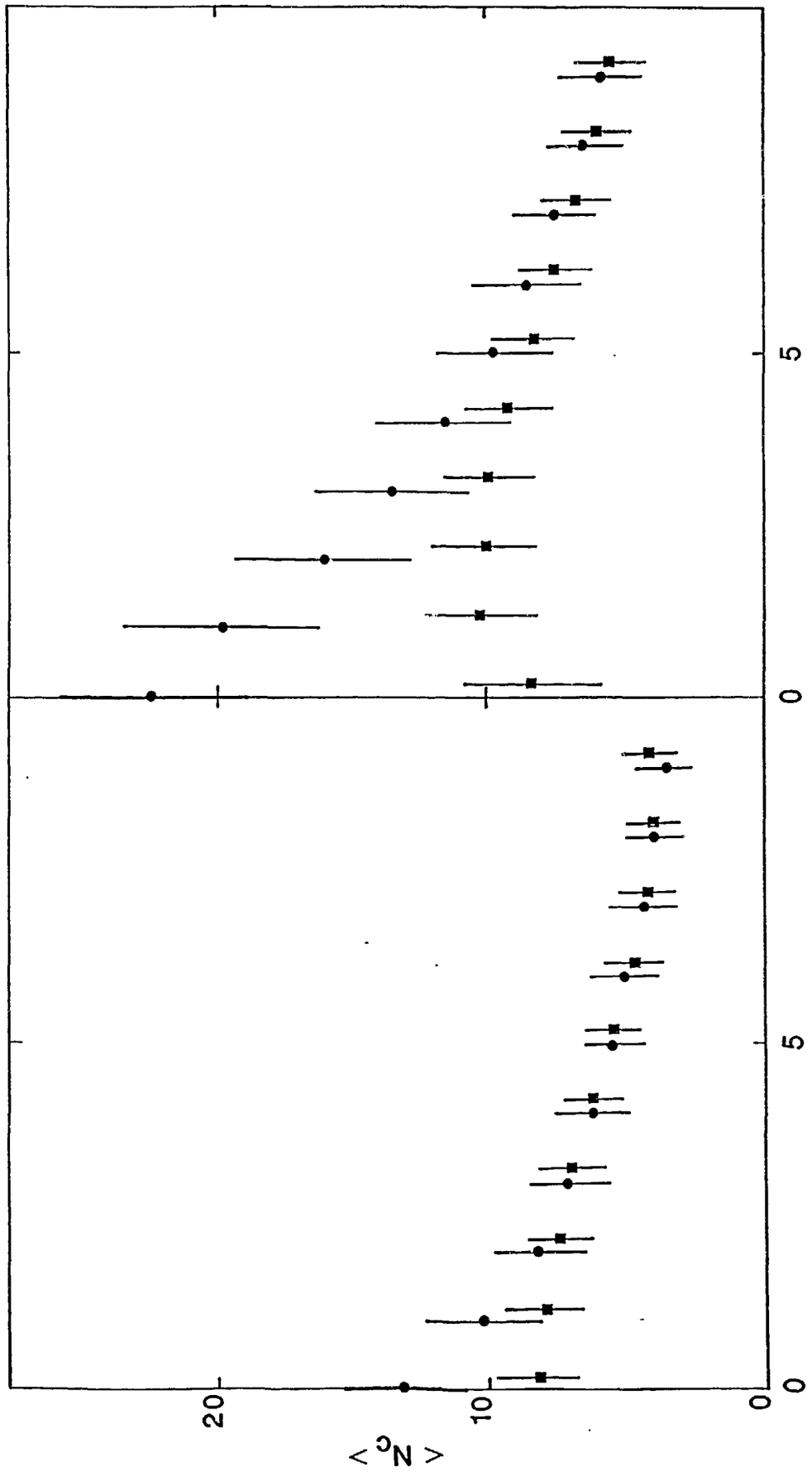


FIG.3

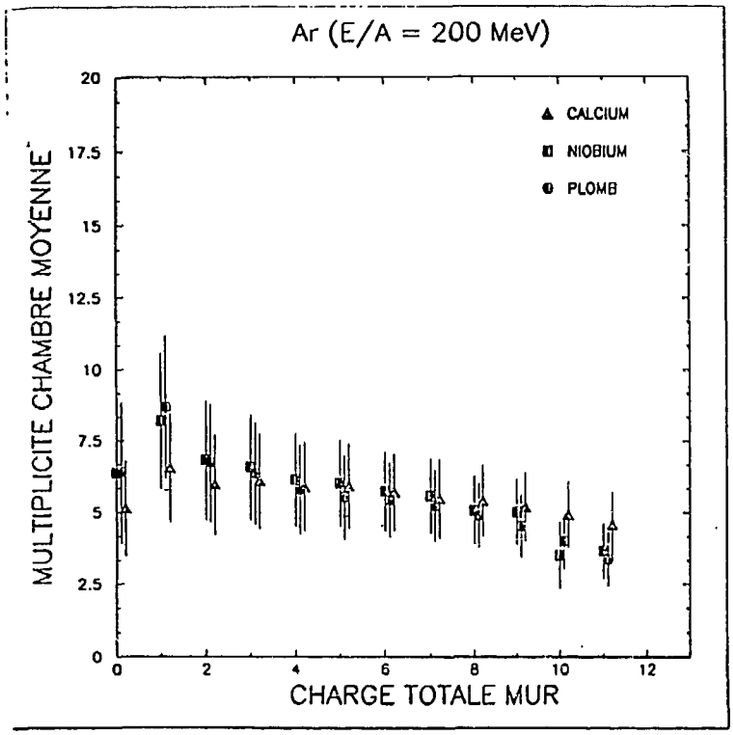
Ar (E/A = 200 MeV)
MULTIPLICITE CHAMBRE MOYENNE
CHARGE TOTALE MUR
CALCIUM
NIOBIUM
PLOMB

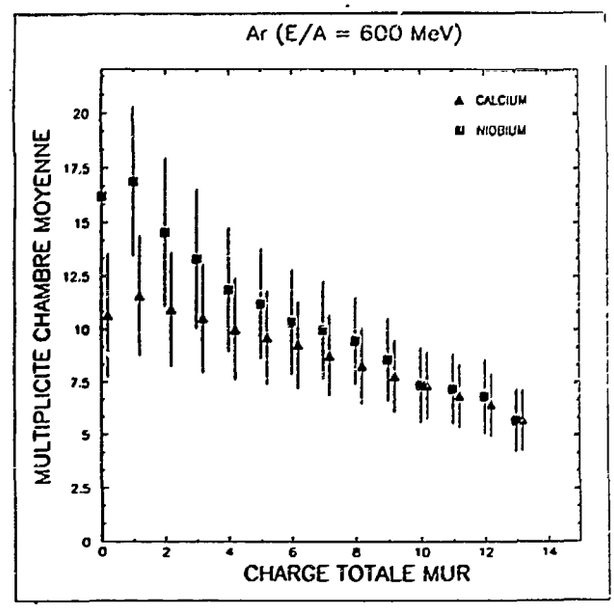
Ar (E/A = 600 MeV)
MULTIPLICITE CHAMBRE MOYENNE
CHARGE TOTALE MUR
CALCIUM
NIOBIUM

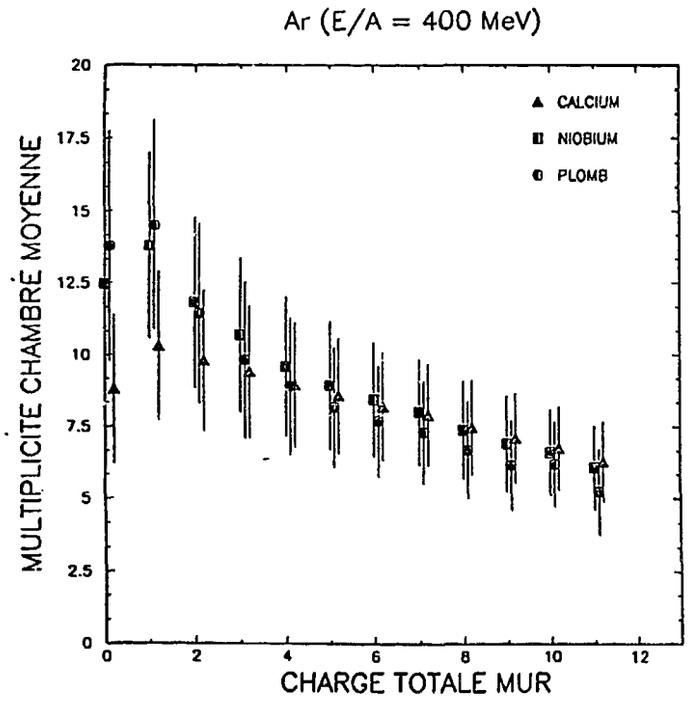
Ar (E/A = 400 MeV)
MULTIPLICITE CHAMBRE MOYENNE
CHARGE TOTALE MUR
CALCIUM
NIOBIUM
PLOMB

FIG. 4

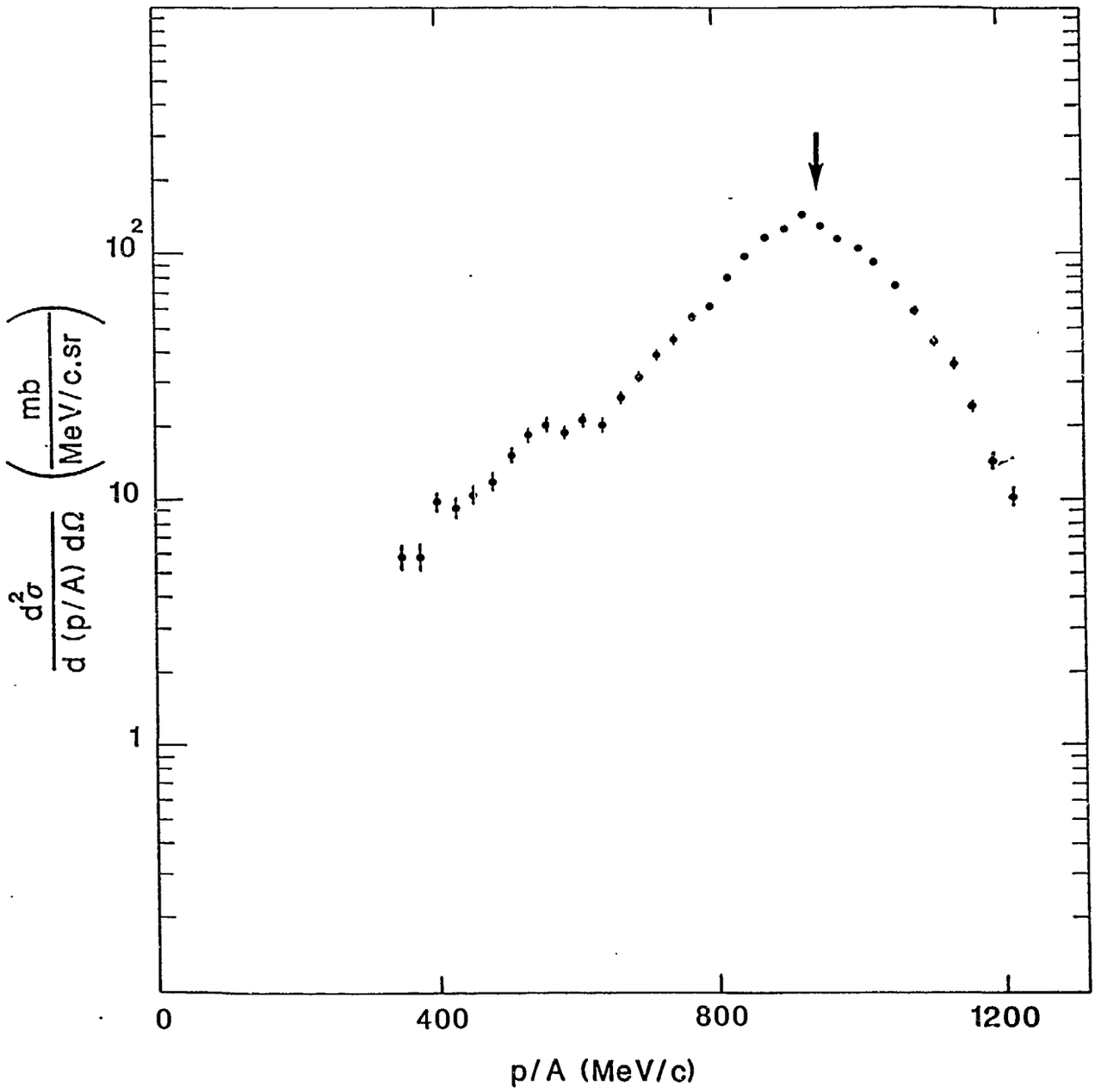
$\frac{d^2\sigma}{d\,(p/A)\,d\Omega}\left(\frac{mb}{MeV/c.sr}\right)$
$10^2$
10
1
0
400
800
1200
p/A (MeV/c)

FIG.5

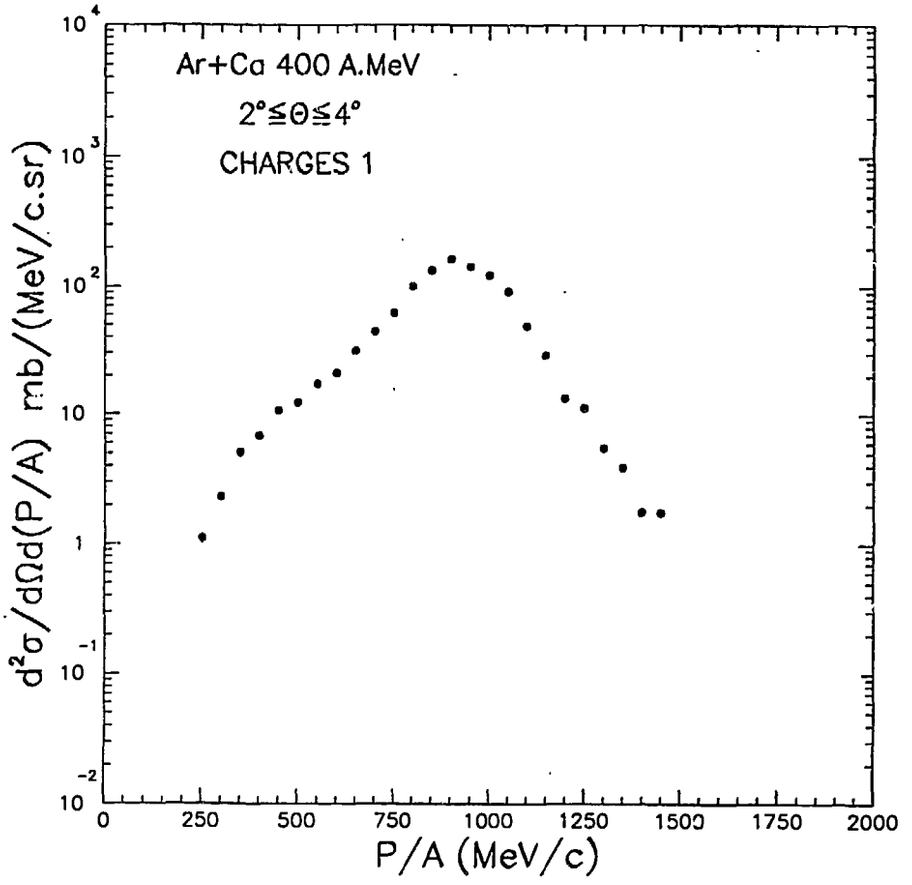
Ar+Ca 400 A.MeV
2°≦Θ≦4°
CHARGES 1
d²σ/dΩd(P/A) mb/(MeV/c.sr)
P/A (MeV/c)

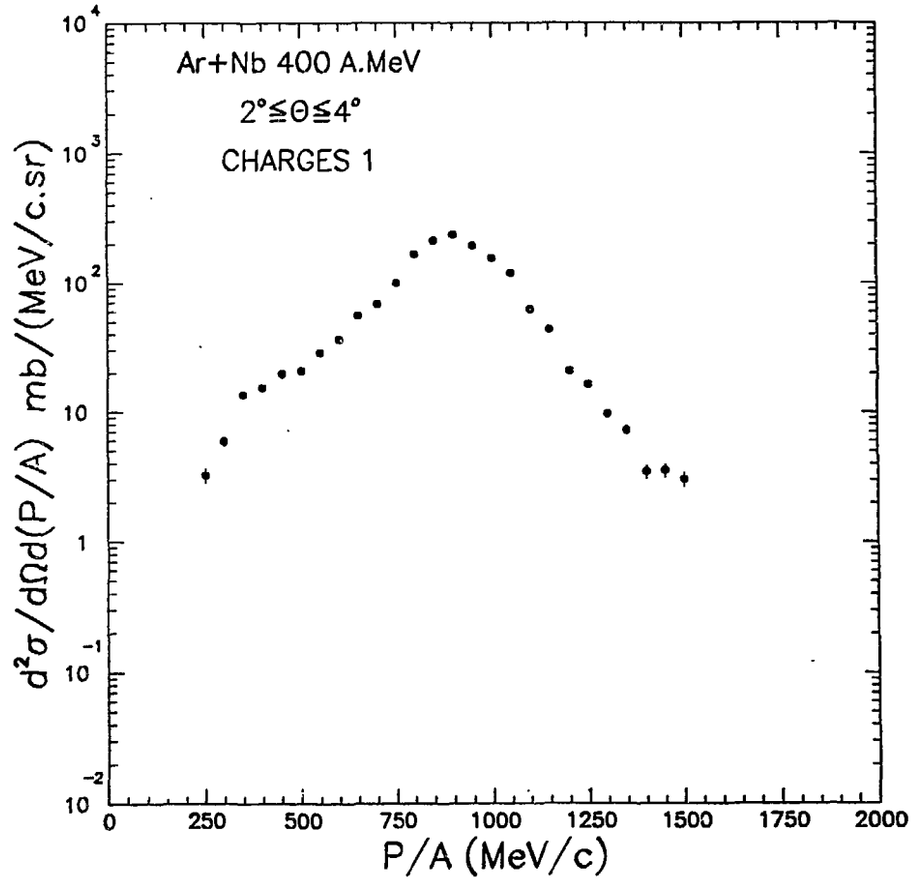
Ar+Nb 400 A.MeV
2°≦Θ≦4°
CHARGES 1
d²σ/dΩd(P/A) mb/(MeV/c.sr)
P/A (MeV/c)

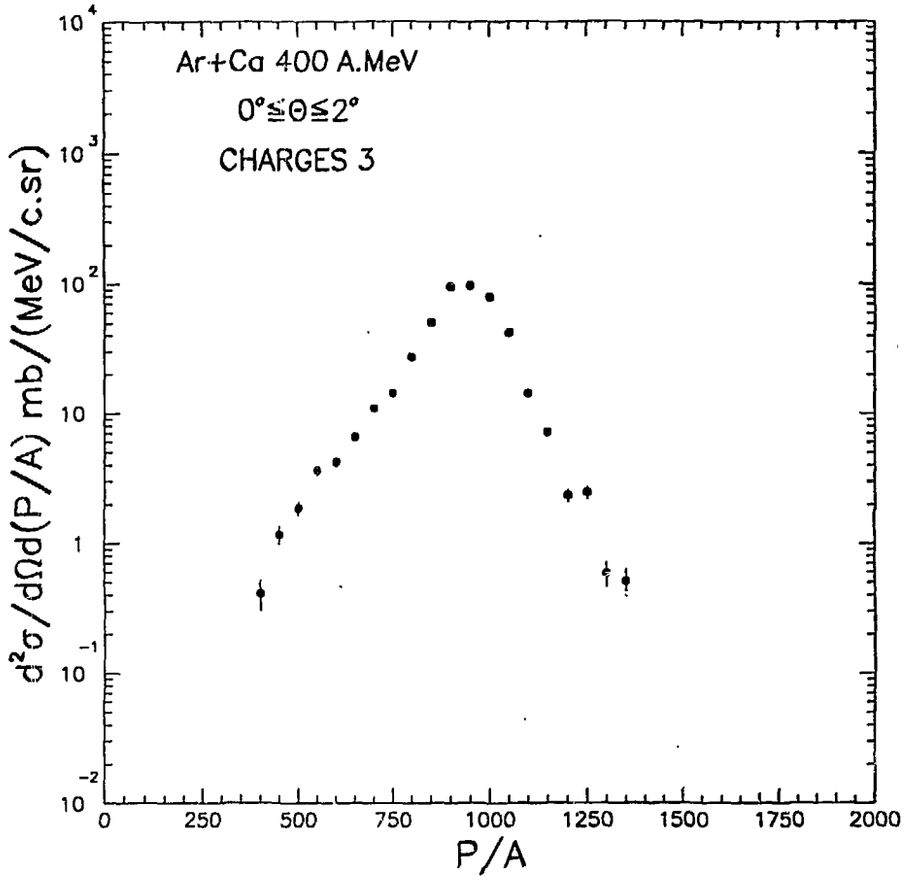
Ar+Ca 400 A.MeV
0°≤Θ≤2°
CHARGES 3
$d^2\sigma/d\Omega d(P/A)$ mb/(MeV/c.sr)
P/A

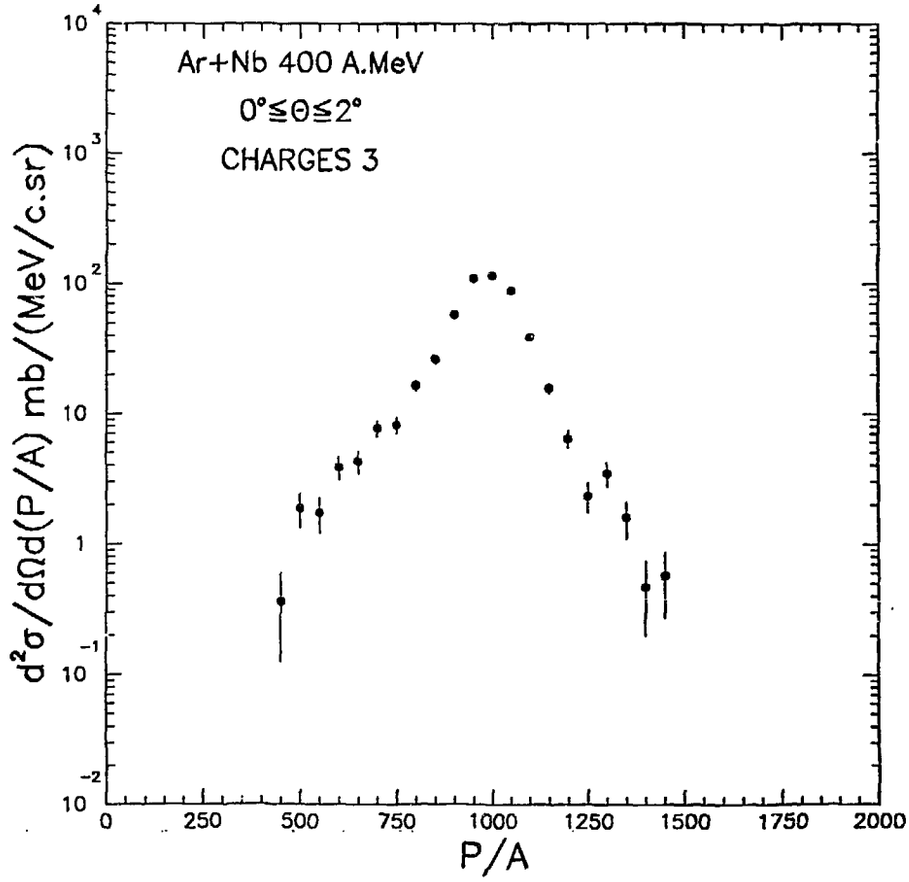
Ar+Nb 400 A.MeV
0°≤Θ≤2°
CHARGES 3
$d^2\sigma/d\Omega d(P/A)$ mb/(MeV/c.sr)
P/A

FIG.7

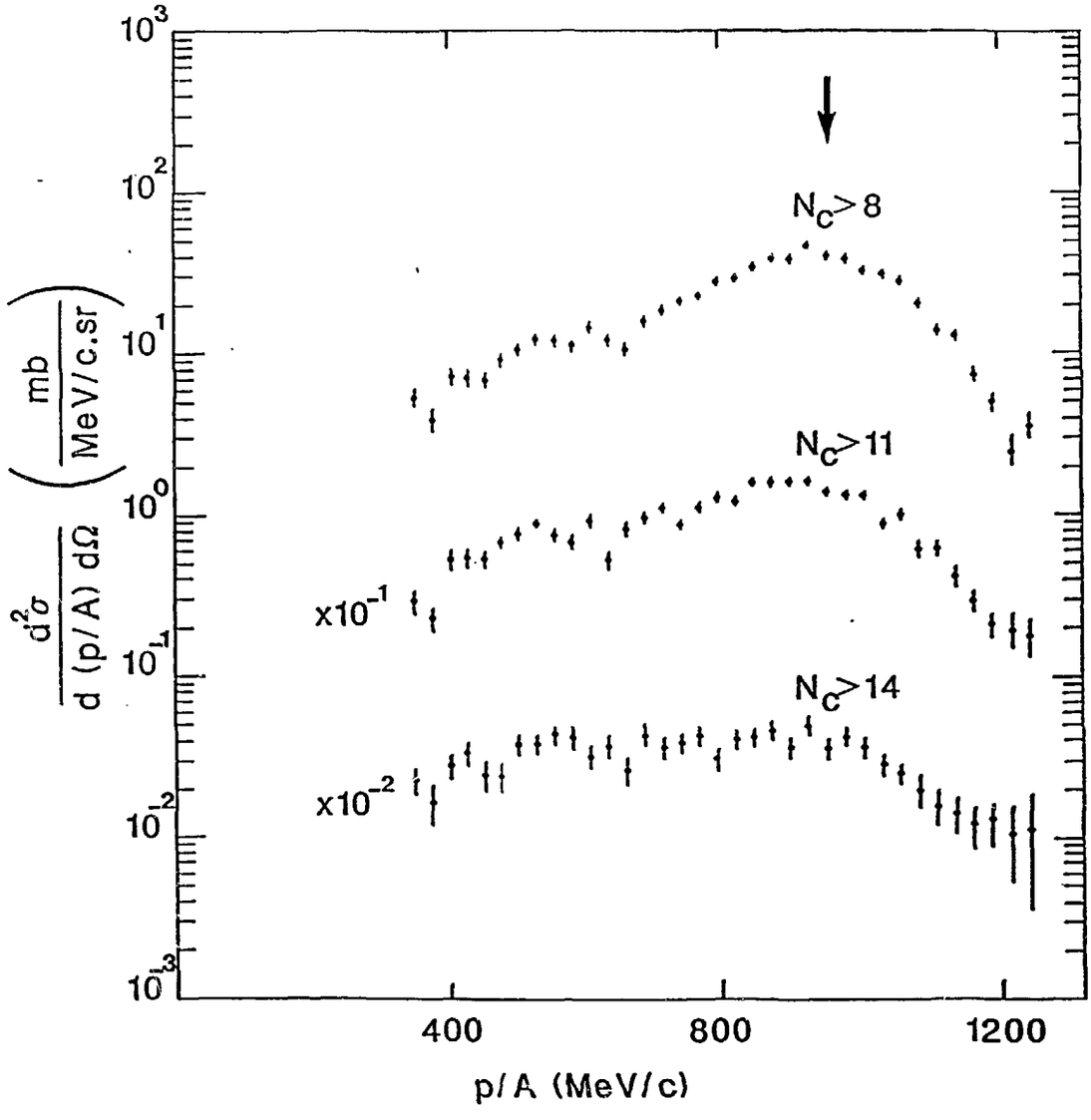
$\frac{d^2\sigma}{d\,(p/A)\,d\Omega}\left(\frac{mb}{MeV/c.sr}\right)$
$10^3$
$10^2$
$10^1$
$10^0$
$10^{-1}$
$10^{-2}$
$10^{-3}$
$N_C > 8$
$N_C > 11$
$N_C > 14$
$x10^{-1}$
$x10^{-2}$
400
800
1200
p/A (MeV/c)

FIG.8

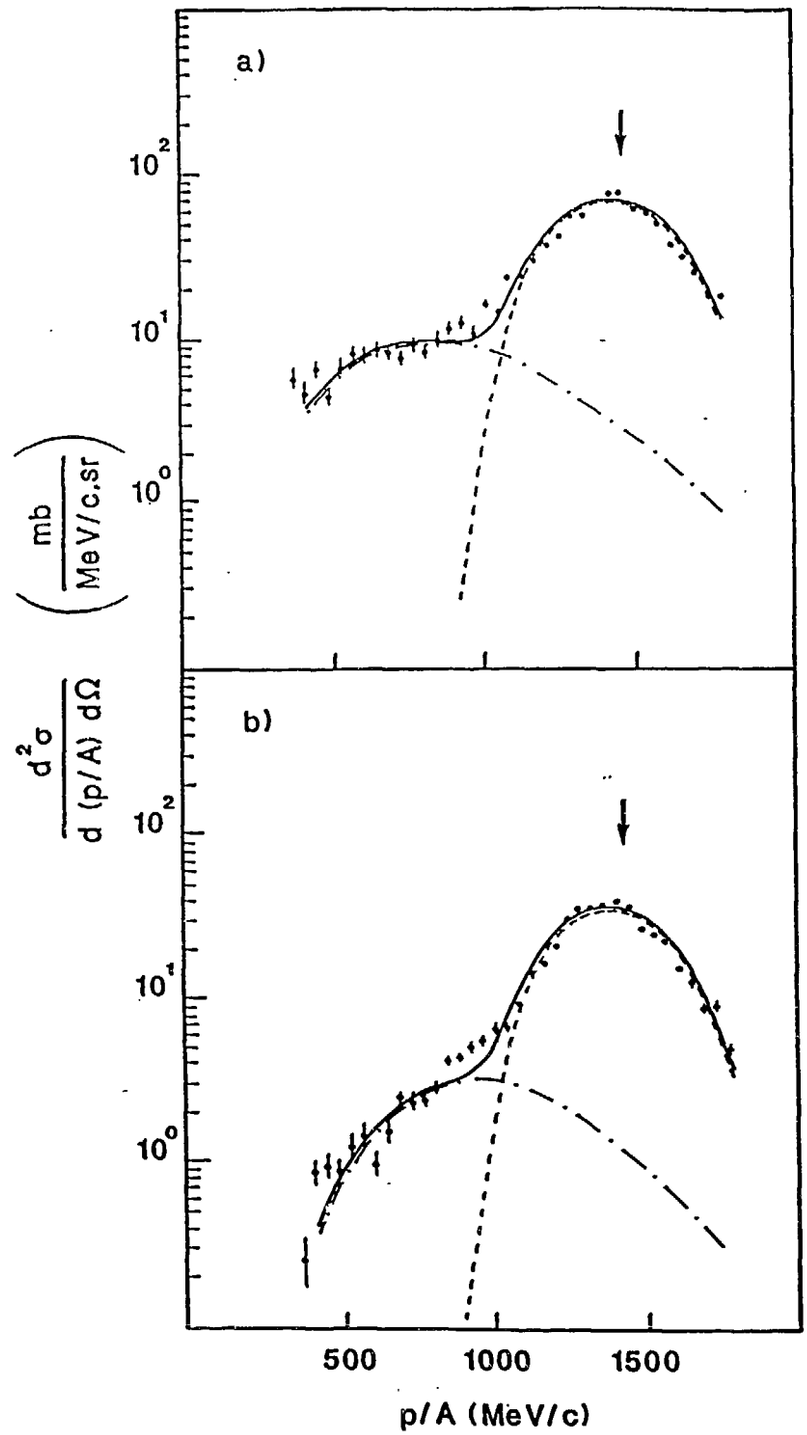
a)
b)
$10^2$
$10^1$
$10^0$
$\frac{d^2\sigma}{d\,(p/A)\,d\Omega}\left(\frac{mb}{MeV/c.sr}\right)$
500
1000
1500
p/A (MeV/c)

FIG.9

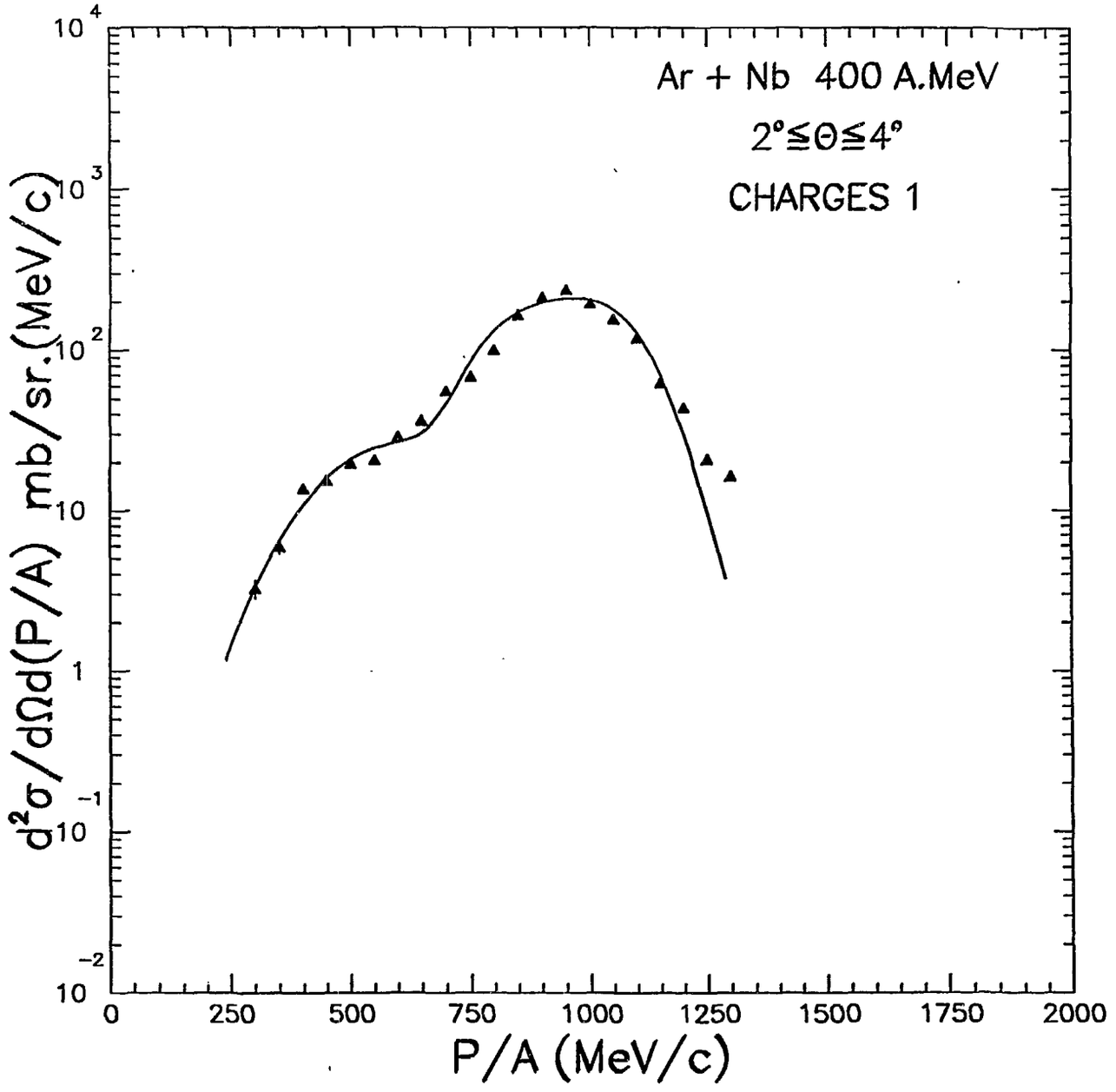
Ar + Nb 400 A.MeV
2°≦Θ≦4°
CHARGES 1
$d^2\sigma/d\Omega d(P/A)$ mb/sr.(MeV/c)
P/A (MeV/c)
$10^4$
$10^3$
$10^2$
10
1
$10^{-1}$
$10^{-2}$
0
250
500
750
1000
1250
1500
1750
2000

FIG.10